UV LASER-INDUCED DOMAIN INHIBITION: A ROUTE TO DOMAIN-ENGINEERED STRUCTURING OF LITHIUM NIOBATE

C. L. Sones[1], Y. J. Ying[1], S. Mailis[1], R. W. Eason[1], H. Steigerwald[2], T. Jungk[2], A. Hoffmann[2], K. Buse[2], E. Soergel[2]
[1]Optoelectronics Research Centre, University of Southampton, Southampton, SO17 1BJ, U.K.
[2]Institute of Physics, University of Bonn, Wegelerstrasse 8, 53115 Bonn, Germany
cls@orc.soton.ac.uk

Abstract: Continuous wave ultraviolet laser irradiation at $\lambda = 244 - 305$ nm of the +z face of congruent and MgO-doped lithium niobate is observed to inhibit ferroelectric domain inversion directly beneath the illuminated region during subsequent electric field poling. When followed by chemical etching, this effect results in creation of high-spatia-resolution domain-engineered microstructures.

1. INTRODUCTION

Domain engineering [1, 2] of ferroelectrics such as lithium niobate (LN) is a subject of extensive research and a simple, cheap, and robust method of fabrication of well-defined periodic domain-inverted structures on submicron scales is highly desirable. The uncontrolled lateral spreading of domains walls associated with the conventional electric field poling technique imposes a lower limit on the scale/size of the spatially engineered domains to values of the order of a few microns.

In an effort to circumvent this limitation, light-assisted domain inversion approaches to achieve micron scale (and ideally the much desired sub-micron scale) domain reversal have recently been the subject of intensive investigation. Previous works have shown that ultraviolet (UV) [3] and visible laser light [4-7] can either directly invert domains or assist the domain inversion process in LN. In this paper however, a contrasting effect [8] is presented wherein illumination of the +*z* face with UV light (with photon energy greater than the LN band gap), instead *inhibits* domain inversion in illuminated areas during subsequent electric field poling (EFP). This effect provides a relatively uncomplicated means for producing periodically domain inverted crystals. Also, if subsequently followed by wet chemical etching which exploits the differential etching characteristics of polar faces of LN, the poling-inhibited domain patterns can then be transformed to produce single domain 2D surface relief structures such as ridges and discs, which can form the building blocks for the fabrication of several interesting integrated optical devices.

In this contribution we will present results that show the applicability of this effect in the creation of high-spatial-resolution micro/nano structures in LN.

2. EXPERIMENTS AND RESULTS

2.1. Scanning with focused beams

The UV light source used for the illumination of the +z face of the LN crystals was a frequency-doubled Ar-ion laser that was focused to a spot size of ~ 2.5 μm. The initial experiments were performed with $\lambda = 244$ nm, however, recent experiments showed that inhibition of poling is also possible by using longer UV wavelengths directly available from an Ar-ion laser (275 – 305 nm). The majority of the results presented here are for $\lambda = 244$ nm. Control over the appropriate positioning and exposure was achieved by a computer-controlled three-axis stage system and a mechanical shutter. Sets of parallel lines were drawn on the crystals along the crystallographic *x* or *y* directions by moving the stages at speeds ranging from 0.05 – 0.3 mm s^{-1}. Arrays of static (dot) exposures, illuminated with exposure times ranging from a few milliseconds to a few tens of seconds, were also performed. The separation between the edges of adjacent illuminated spots in the arrays varied from 0 – 6 μm. This permitted us to verify the presence of any proximity effect observed in [3] between adjacent poling-inhibited domains. For both, dynamic and static exposures, the power was varied between 20 – 28 mW.

The UV irradiated samples were subsequently poled using the EFP setup described in Ref. 5. The voltage was ramped at 2 kV/min to a value of ~ 10.1 kV, corresponding to an electric field of 20.2 kV/mm across the 0.5 mm thick sample. This value of the applied electric field ensures that domain inversion occurs slowly, which is desirable since it was observed that the kinetics of the domain wall motion is seen to influence greatly the shape and quality of the resultant poling-inhibited domain structures.

Finally, etching of the crystals in aqueous HF acid solution results in the delineation of the 2D surface relief structures through the differential etch rates [9] of the two polar z-faces. Longer etching times produce high-aspect-ratio 3D structures such as ridges and ultra-sharp tips. Furthermore, piezoresponse force microscopy (PFM) [10] was also used to validate the domain nature of these poling-inhibited structures.

The smooth, continuous ridges (Fig. 1a) and discs (Fig. 1b) correspond to the UV illuminated areas of

the crystal face that have maintained their original domain orientation. The rough background corresponds to the newly domain inverted –z-face area, which has been etched and consequently appears rough.

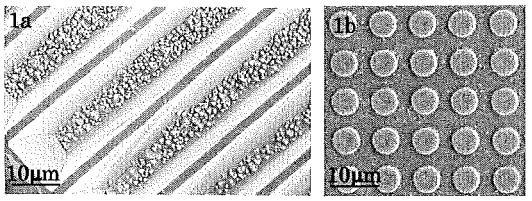

Fig. 1: SEM pictures of ridges (a) and discs (b) formed by the corresponding UV ($\lambda = 244$ nm) illumination patterns followed by EFP and etching.

If the samples are allowed to etch for longer periods of time, then this leads to the formation of high aspect ratio structures as shown in Fig. 2. These structures have resulted as a consequence of prolonged room temperature etching over a period of 39 hrs for the case of lines in Figs. 2a and 2b, and 21 hrs for the case of tips in Figs. 2c and 2d. The higher magnification SEM images in Figs. 2b and 2d show the quality of the etched facets shaped via this route. The samples were tilted by 45° during the SEM imaging which allowed the observation of the quality of the sidewall of the poling-inhibited domain. This underlines the potential of this method for surface micro-structuring.

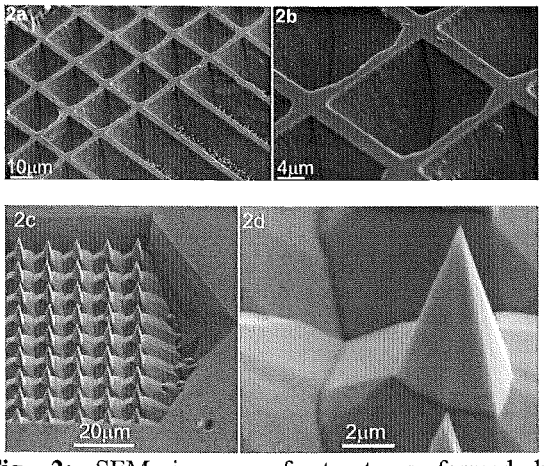

Fig. 2: SEM images of structures formed by prolonged etching of poling-inhibited lines and discs. Illumination was at $\lambda = 244$ nm.

2.2. Two beam interference

A two-beam interference experimental arrangement which allowed submicron periodic exposures over larger areas of the crystal via single exposures was also investigated. The incident interference fringe pattern imposed on the surface of the crystal had a period of 700 nm and extended over an area of around 2000 μm^2. As with previous experiments, several different exposure times, ranging from tens of milliseconds to tens of seconds, and a range of incident laser powers were used.

Interferometric exposures were done at much lower laser intensity than single beam exposures due to the experimental restrictions which only allowed a large spot size. A single spherical lens was used to focus two incident parallel beams on the common focal point where they could interfere. The fringe spacing was determined by the initial separation of the two parallel beams. In such an arrangement the beams do not propagate paraxially through the lens hence aberrations are introduced which did not allow tight focusing. A periodic surface relief structure produced on exposure of the $+z$ face followed by bulk EFP and etching is shown in the SEM image of Fig. 3. The structure which is shown in this SEM image is qualitatively different to the ones produced using higher intensities. However, PFM measurements showed that the surface relief pattern shown in Fig. 3, as revealed by chemical etching, is a single domain structure. This might have originated by a periodic poling-inhibited structure which has been removed by the acid. Due to the low intensity used here as compared to the single beam experiments, the initial poling-inhibited areas are expected to be very narrow and shallow hence easily removed by the acid via side etching. However, they resist etching long enough to produce a surface relief pattern. By using higher UV laser intensities it is expected that deeper periodic domain structures can be fabricated at the highly desired sub-micron scale.

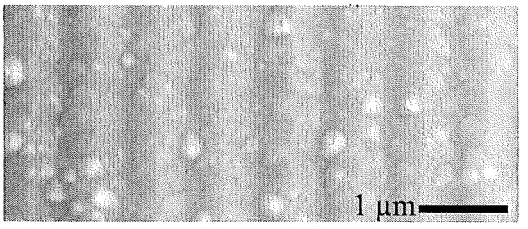

Fig. 3: SEM image of the periodic structure formed by interferometric exposure with ($\lambda = 244$ nm).

2.3. Spatial resolution

Arrays of discs like the ones shown in Figs. 4 and 1b were produced by static (dot) exposures and can have arbitrary dot separations. No interaction between adjacent poling-inhibited dots was observed even when the separation between them was less than one micron (Fig. 4b). However, when the illuminated areas overlapped, the regions of poling-inhibited domain inversion merged. This can be seen on the left hand side of Fig. 4a, where stage backlash distorted the array by reducing the dot spacing. Additional UV exposure of a specific area was not observed to produce any further effect. This can also be observed in the cross-hatched pattern shown in Figs. 2a and 2b, which is a result of sequential line scans along the x and y crystallographic axes. These cross-hatched patterns hence correspond to double exposures.

The potential of this technique to form precisely positioned structures without proximity restrictions

demonstrates the practicality of this technique in the implementation of devices such as couplers, y junctions, ring micro-resonators, and photonic crystals.

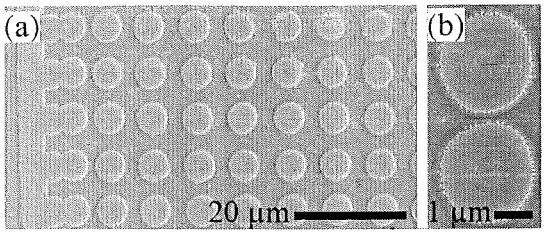

Fig. 4: SEM image of a dot array. Illumination was at $\lambda = 244$ nm.

The width of the area over which inhibition occurs is seen to be dependent upon both the incident power and the dwell time (scanning speed) of the beam with larger domains formed with longer dwell times (which correspond to lower scan speeds). This functionality reiterates the capability of this technique in being able to achieve further control over the shape and size of the structures that can be produced.

The quality of the poling-inhibited regions was observed to depend upon the domain wall kinetics during the EFP step. It was seen that when the wall movement was smooth and reasonably slow, the inhibition process produced continuous domains. In congruent crystals when the wall movement can be fast, expanding in a 'jerky' manner [2, 11], the poling-inhibited regions appeared fragmented or did not exist at all in areas corresponding to fast domain wall motion. In the MgO-doped crystals where EFP is known to be slower and smoother [12, 13], the poling-inhibited domains appeared to be smooth and continuous everywhere.

2.4. Stability

In order to investigate the stability of the poling-inhibited domains, the crystal was thermally annealed for 1 hr at 215°C after the EFP step of the process. SEM investigation of the HF-etched annealed crystal showed that the poling-inhibited domains survived the brief annealing process without any significant change apart perhaps from the fact that after annealing there seems to be a slight improvement on the quality of the domain edges.

2.5 Poling depth

The nature and orientations of the poling-inhibited domains was also investigated by PFM which confirmed the observations deduced from chemical etching. Figure 5 shows a PFM image of an area of the crystal that carries a set of static dot illuminations and has also subsequently been partially poled (only a fraction of the exposed area was domain inverted).

Full contrast in this image is associated with opposite ferroelectric bulk domains. In the image shown in Fig. 5, a $+z$ face appears white (left section of the image) while a $-z$ face appears black (right larger section of the image). The bright dots in a black background of the PFM image correspond to the UV exposed areas which have maintained their original domain orientation ($+z$) while the surrounding area has been inverted ($-z$). The fact that the dots show full PFM contrast underlines that the depth of the poling-inhibited structures must be > 300 nm [14].

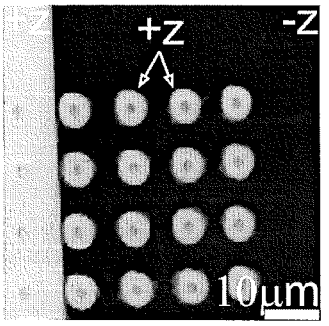

Fig. 5: PFM image of partially poling-inhibited dot array. White = $+z$ face, black = $-z$ face as indicated. White area to left of image is an un-poled bulk domain.

The depths of the poling-inhibited domain structures were further investigated by y-face etching. In the case of the structures formed for an illuminating wavelength of 244 nm the etched y-face indicated that the depths of the poling-inhibited domains were in the range of ~ 2.5 μm. For implementation of such poling-inhibited domain structures for integrated optical waveguide interactions greater depths exceeding the value (up to ~ 5 μm) would be ideal. In an attempt to overcome this limitation we investigated the process using a range of longer wavelengths (275, 300.3, 302 and 305 nm). These wavelengths were available from the Ar-ion laser. Additionally, as at these longer wavelengths the corresponding absorption coefficients are smaller, being closer to the UV absorption edge of LN, the 1/e absorption depth of the laser light extends to greater depths, and this should therefore translate to proportionally deeper domains. As expected, the effect was observed for the whole range of wavelengths used. Inhibition of poling was indeed observed for a wide range of exposure conditions. For these wavelengths the laser power used ranged from 35-60 mW, while the scanning speed range was kept the same as in the 244 nm exposure case.

Preliminary domain depth measurements (by y-face etching) for these samples exposed with longer wavelength showed that the corresponding values of the poling-inhibited domain depths was slightly deeper when compared to those for 244 nm, and were in the range of ~ 2.5–5 μm.

2.6. Refractive index change

Direct writing with c.w. UV [15, 16] light at 244 nm wavelength is known to induce under certain

conditions a refractive index change underneath the written z-faces of LN crystals which is sufficient for the formation of optical waveguides. Since the first step in the domain structuring route described here is UV irradiation of crystal faces, it is expected that a refractive index change would also be present in the poling-inhibited structures. Waveguide propagation was indeed observed through a ridge structures similar to those shown in Fig. 1a. Hence, it is possible to combine refractive index structures along with ferroelectric domain and physical structures, which increases the flexibility and applicability of this method for the fabrication of integrated-optical devices.

2.7. Proposed mechanism

The origin of the observed inhibition of domain reversal can be attributed to the presence of an electrostatic charge distribution under the crystal surface induced by the UV laser irradiation [8]. This charge distribution poses an electrostatic barrier which stops the propagation of a bulk inverted ferroelectric domain during EFP. This charge distribution is produced by a combination of photo-excited charges produced via the combination of UV laser illumination, and heating of the crystal [16]. A pyroelectric field is formed which drives electrons into the bulk of the crystal and holes toward the surface (for the +z face illumination case) which become subsequently fixed in the absence of light and heat after the UV beam is removed. During EFP, ferroelectric domains which nucleate on the –z face and propagates toward the +z face, get influenced by the electrostatic barrier which has been established by the UV irradiation and are diverted, thus leaving the volume immediately below the UV irradiated area in its original domain orientation. Macroscopically this appears as a local increase of the coercive field. This mechanism has some similarities to that described by Dierolf and Sandmann [4] for confocal light-assisted poling. However, in the effect which is discussed here the driving field for the electrons is the pyroelectric field rather than an external electric field, and is opposing local domain inversion rather than enhancing it. Finally, the mechanism we describe is latent and does not require application of the external field during illumination.

3. CONCLUSIONS

As a method of surface structuring, UV poling inhibition followed by etching is simple, inexpensive and flexible to implement. The shape/size and the quality of the fabricated structures is determined by the incident exposure conditions, in combination with the subsequent EFP parameters and the annealing steps respectively. Additionally, as the crystallographic symmetry is not observed to impose limitations on the orientations of the created structures, any desired shapes can be achieved. Also the single domain nature of these structures provides the necessary requirement for implementation of efficient nonlinear, piezoelectric and other domain-orientation-sensitive devices.

ACKNOWLEDGEMENT

The authors are grateful to the Engineering and Physical Sciences Research Council, UK for research funding under grant no. EP/C515668, the EU research funding under Grant No. EP/C515668 and STREP 3D-DEMO respectively and the Deutsche Forschungsgemeinschaft for the grant BU913/18.

REFERENCES

[1] B. J. Rodriguez, R. J. Nemanich, A. Kingon, A. Gruverman, S. V. Kalinin, K. Terabe, X. Y. Liu and K. Kitamura, Applied Physics Letters **86**, 012906 (2005).

[2] V. Y. Shur, Ferroelectrics **340**, 3 (2006).

[3] I. T. Wellington, C. E. Valdivia, T. J. Sono, C. L. Sones, S. Mailis and R. W. Eason, Applied Surface Science **253**, 4215 (2007).

[4] V. Dierolf and C. Sandmann, Applied Physics Letters **84**, 3987 (2004).

[5] C. L. Sones, M. C. Wengler, C. E. Valdivia, S. Mailis, R. W. Eason and K. Buse, Applied Physics Letters **86**, 212901 (2005).

[6] M. Müller, E. Soergel and K. Buse, Applied Physics Letters **83**, 1824 (2003).

[7] M. C. Wengler, U. Heinemeyer, E. Soergel and K. Buse, Journal of Applied Physics **98**, 064104 (2005).

[8] C. L. Sones, A. C. Muir, Y. J. Ying, S. Mailis, R. W. Eason, T. Jungk, A. Hoffmann and E. Soergel, Applied Physics Letters **92**, 072905 (2008).

[9] C. L. Sones, S. Mailis, W. S. Brocklesby, R. W. Eason and J. R. Owen, J. Mater. Chem. **12**, 295 (2002).

[10] T. Jungk, A. Hoffmann and E. Soergel, Applied Physics Letters **89**, 163507 (2006).

[11] V. Gopalan, Q. X. Jia and T. E. Mitchell, Applied Physics Letters **75**, 2482 (1999).

[12] A. Kuroda, S. Kurimura and Y. Uesu, Applied Physics Letters **69**, 1565 (1996).

[13] K. Nakamura, J. Kurz, K. Parameswaran and M. M. Fejer, Journal of Applied Physics **91**, 4528 (2002).

[14] T. Jungk, A. Hoffmann and E. Soergel, New Journal of Physics **10**, 013019 (2008).

[15] I. T. Wellington, S. Mailis, C. B. E. Gawith, G. J. Daniell, P. G. R. Smith and R. W. Eason, presented at the Conference on Lasers and Electro-Optics (CLEO), San Francisco, CA, USA, 2004.

[16] A. C. Muir, G. J. Daniell, C. P. Please, I. T. Wellington, S. Mailis and R. W. Eason, Applied Physics A-Materials Science & Processing **83**, 389 (2006).